

# Friction factor evaluation by FEM and experiment for TA15 titanium alloy in isothermal forming process

Da-Wei Zhang · He Yang · Hong-Wei Li ·  
Xiao-Guang Fan

Received: 27 March 2011 / Accepted: 31 August 2011 / Published online: 23 September 2011  
© Springer-Verlag London Limited 2011

**Abstract** The friction at die–workpiece interface is an important parameter in metal forming processes, which affects the metal flow, cavity fill, surface quality, etc. The friction in the forming process is influenced by material properties and forming conditions. The friction in forming process of TA15 (Ti–6Al–2Zr–1Mo–1V) titanium alloy under high temperatures (isothermal forming) and low strain rates is studied here by ring compression test. The friction calibration curves are elaborated by means of finite element method. The research on the calibration curves and friction factor at the loading speed  $v=0.1\text{--}1.0$  mm/s and the conventional forging temperature (950°C) and near-beta forging temperature (970°C) is carried out. The influence of loading speed on friction calibration curves is similar to the influence on friction factor  $m$ : at the low ( $m < \text{about } 0.1$ ) or high ( $m > \text{about } 0.7$ ) friction condition, the influence of loading speed can be ignored, however the influence is notable in the midst magnitude (about 0.2–0.5). The temperature variation from 950°C to 970°C has little influence on friction calibration curves, but has notable influence on  $m$  under lubricated condition.

**Keywords** Shear friction factor · Ring compression test · Calibration curves · Finite element method · TA15 titanium alloy

## 1 Introduction

Titanium and titanium alloys are a kind of important material in aviation, aerospace, marine, and automobile industry fields due to high specific strength, excellent corrosion resistance, good weldability, and high temperature performance [1–3]. Several metal forming manners, such as cold forming, warm forming, hot forming, etc., are employed in plastic forming filed of titanium and its alloys [4–10]. Isothermal forming (high temperature) may allow near-net forming of large-scale complex titanium alloy components, which often serve as the key load-bearing components under severe working conditions. Friction is one of the most significant factors in metal forming process, which affects metal flow, workpiece integrity and surface finish, cost considerations, and energy conservation [11–15]. Especially the isothermal forming process of titanium alloy is sensitive to the friction. Thus, it is necessary to quantitatively evaluate the magnitude of friction under the operation conditions in order to optimize the isothermal forming process of titanium alloy component.

The constant shear friction model is used in most research on hot forming, and the shear friction model has been widely used in simulations of bulk metal forming due to its theoretical simplicity and numerical rigidity [15, 16]. However, the detailed measurement and investigation of friction in metal forming are not easy due to the high pressure, the high temperature, and the complex nature of the interrelationships between the great varieties of parameters involved, especially for the hot metal forming [12, 15]. The ring compression test is a proven test to determine friction factor  $m$ , with which the friction is measured without knowing the force of the deformation and the flow stress of material [17, 18]. In order to obtain the magnitude of friction, the change in inner diameter of the compressed

D.-W. Zhang · H. Yang · H.-W. Li · X.-G. Fan  
State Key Lab of Solidification Processing, School of Materials  
Science and Engineering, Northwestern Polytechnical University,  
Xi'an 710072, People's Republic China

D.-W. Zhang (✉) · H. Yang · H.-W. Li · X.-G. Fan  
Northwestern Polytechnical University,  
127 You Yi West Rd., P.O. Box 542, Xi'an, Shaanxi 710072,  
People's Republic China  
e-mail: zhangdawei2000@yahoo.com.cn

ring must be compared with the specific curves called calibration curves which are the relationships between the inner diameter and height of the ring during the deformation under various friction factors.

The material properties and forming conditions play an important role in the shape of the calibration curves [19, 20]. Sofuoğlu and Rasty [19] studied the friction calibration curves of black plasticine and white plasticine and presented that the use of friction calibration curves regardless of the material type and forming conditions must be avoided. In order to provide the same value of friction factor in both real and physical simulation of bulk metal forming, the ring compression test with plasticine and lead under various lubricants and friction conditions were performed, and a full range of friction conditions were obtained to model for the physical simulation [20]. Rudkins et al. [21] investigated the friction of steel in hot forming by using the ring compression test. By using the ring compression test, Li et al. [22, 23] studied the lubricities of glass and graphite in deformation process of Ti–6Al–4V titanium alloy under high temperatures (750°C, 800°C, 850°C, 950°C, 1,000°C) and strain rates (0.05, 0.5, 5, 15 s<sup>-1</sup>), and presented that increasing the strain rate leads the friction to reduce. However, the influence of material properties and forming conditions on the calibration curves is not considered in the above studies [20–23] although Fereshteh-Saniee et al. [20] presented that shape of the calibration curves may depend on the material properties. In order to address the dependency of the calibration curves on the parameters such as material properties, relative velocity, and barreling, the numerical method such as the finite element method (FEM) is used to elaborate the friction calibration curves [15, 19].

TA15 (Ti–6Al–2Zr–1Mo–1V) titanium alloy has extensive application in aircraft and aerospace field. The isothermal forming process of titanium alloy is often carried out under low strain rate. In general, the loading speed  $v=0.1\text{--}1.0$  mm/s (the strain rate  $\dot{\epsilon}=0.015\text{--}0.250$  s<sup>-1</sup> in the ring compression test) is used in the industrial forming process. The research on the friction factor in bulk forming of titanium alloy is little except the research on Ti–6Al–4V titanium alloy with graphite and glass [22, 23]. However, the influence of material properties and forming conditions on the calibration curves is not considered by Li et al. [22, 23]. TA15 titanium alloy is a near-alpha titanium alloy and Ti–6Al–4V titanium alloy is a ( $\alpha+\beta$ ) titanium alloy. The forming conditions (strain rates are about 0.015–0.250 s<sup>-1</sup>, and the working temperatures are 950°C and 970°C) in the present study are also different from the forming conditions (strain rates are 0.05, 0.5, 5, 15 s<sup>-1</sup>, and the working temperatures are 750°C, 800°C, 850°C, 950°C, 1,000°C) in the study [22, 23]. So, it is necessary to study the friction in TA15 titanium alloy isothermal forming under high

temperature and low strain rate. Thus, this paper is concerned with the friction in TA15 titanium alloy isothermal forming under low loading speed  $v=0.1\text{--}1.0$  mm/s, in which the shear friction model is used. The calibration curves of TA15 titanium alloy ring are elaborated with FEM simulation where material properties and forming conditions are regarded. The ring compression tests under unlubricated condition and with two glass lubricants at conventional forging temperature (950°C) and near-beta forging temperature (970°C) are carried out. The influence of temperature and loading speed on the calibration curves and the shear friction factor under various lubricated conditions are discussed. The results indicate that the influence law of loading speed on friction factor is different to that declared by Li et al. [22, 23]. The reason is that loading speed mainly affects the shape of barreled free surface but does not affect lubricity in lubricant film under high temperature and low strain rate.

## 2 Research method

### 2.1 Material and equipment for experimentation

A TA15 near-alpha titanium alloy is used in this investigation, of which measured beta-transus temperature is 990°C. Based on the isothermal compression experiment at constant strain rate, the relationship between stress and strain of TA15 titanium alloy is acquired in our group [24]. Figure 1 presents the flow stress data with temperature at strain rates 0.01, 0.1, and 1 s<sup>-1</sup>. The initial ring is 21 mm in outer diameter ( $D_0$ ), 10.5 mm in inner diameter ( $d_0$ ), and 7 mm in height ( $H_0$ ), i.e.,  $D_0:d_0:h_0=6:3:2$ .

All the isothermal ring compression tests are performed employing a 200-kN testing machine shown in Fig. 2. The material of upper and lower platens is K403 nickel-base superalloy, which is also the material for the die used in the isothermal forming process of large-scale complex TA15 titanium alloy components.

### 2.2 Experimental conditions

Usually, the isothermal forging of titanium alloy is carried out under low strain rate. For example, in the isothermal local loading process (which is an isothermal forging realized by local loading) of large-scale complex TA15 titanium alloy components, the loading speed is 0.1–0.4 mm/s. In the local loading process of TA15 titanium alloy bulkhead presented in Section 3.2, the loading speed is about 0.2 mm/s. In the isothermal local loading processes of eigenstructures which are put forward from large-scale components and can reflect the forming characteristics of large-scale components, the speed of upper die may come

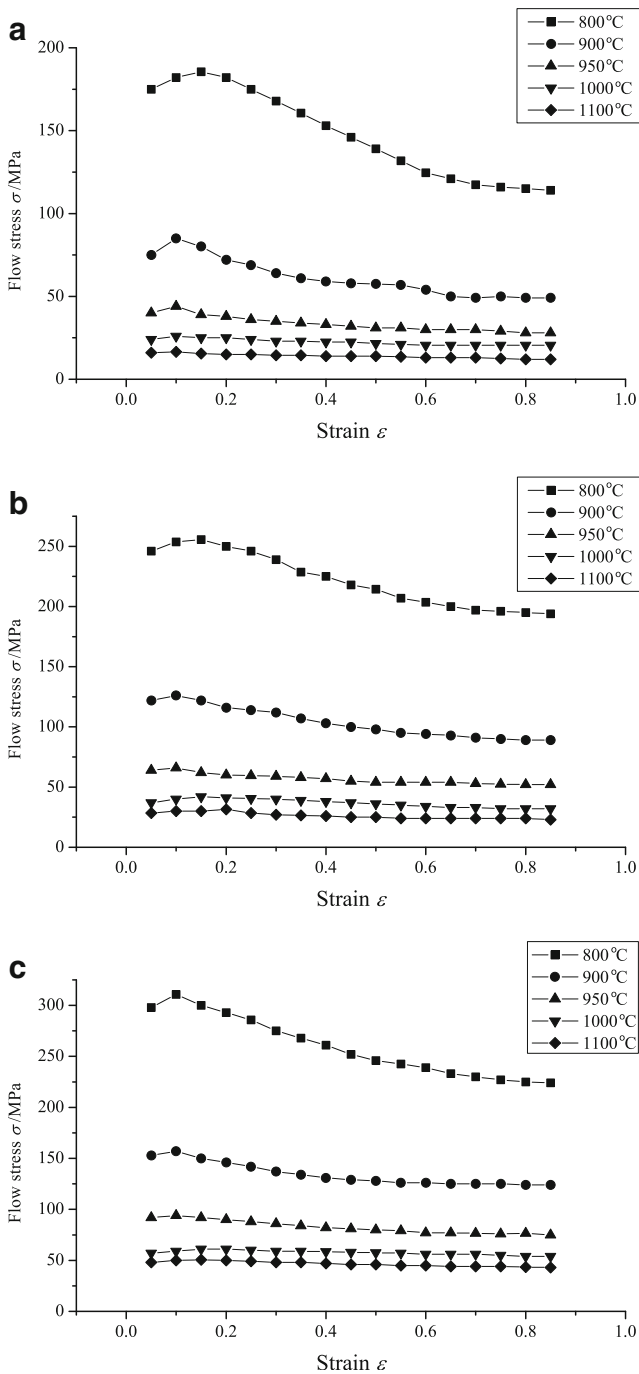


**Fig. 1** Flow stress of TA15 titanium alloy at different temperatures: **a**  $\dot{\epsilon}=0.01 \text{ s}^{-1}$ , **b**  $\dot{\epsilon}=0.1 \text{ s}^{-1}$ , **c**  $\dot{\epsilon}=1.0 \text{ s}^{-1}$

up to 1 mm/s [25]. Sun and Yang [26] presented the optimal forging technique of titanium alloy in multifire forging as follows: adopting conventional forging at first and then following near-beta forging. The working temperature is 950°C for conventional forging and about 970°C for near-beta forging in industrial forming process of TA15 alloy. Thus, the forming temperature  $T=950^\circ\text{C}$  and  $970^\circ\text{C}$  and constant loading speed  $v=0.1, 0.2, 0.5, 0.7,$  and  $1.0 \text{ mm/s}$

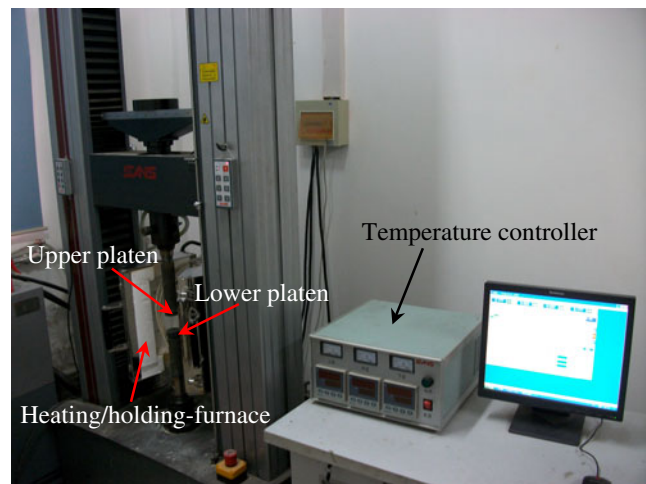


**Fig. 2** The testing machine used for isothermal ring compression tests

are used in the present study. The strain rate in ring compression test is estimated by the method mentioned by Wang et al. [27]:  $\dot{\epsilon}=0.015\text{--}0.025 \text{ s}^{-1}$  at 0.1 mm/s,  $\dot{\epsilon}=0.03\text{--}0.05 \text{ s}^{-1}$  at 0.2 mm/s,  $\dot{\epsilon}=0.075\text{--}0.125 \text{ s}^{-1}$  at 0.5 mm/s,  $\dot{\epsilon}=0.105\text{--}0.175 \text{ s}^{-1}$  at 0.7 mm/s, and  $\dot{\epsilon}=0.15\text{--}0.25 \text{ s}^{-1}$  at 1.0 mm/s.

The glass lubricant is adopted in the isothermal local loading process of large-scale complex components, and it is not only used to lubricate but also used to prevent oxidization. Two glass lubricants (water-based lubricant) are used in the present study: lubricant 1 comes from industrial forming process, of which main components are glass and graphite; lubricant 2 comes from the laboratory, which only includes glass and excludes graphite. Lubricant 1 is used in the industrial forming process of large-scale bulkhead presented in Section 3.2. The ring is lubricated before compression experiment. The lubricated operation is as follows: heating to 150°C and holding for some time; taking out and spraying lubricant; and air cooling to room temperature.

Several ring compression tests are carried out under the same forming conditions (such as temperature, speed, and friction conditions) and are deformed to different reductions in height, which are carried out individually from 25% to 50%. As recommended by Joun et al. [15], the measured inner diameter is the minimum inner diameter  $d_{\min}$ . The inner diameter is measured in three directions, and the average value is used to calculate the percentage change. The reduction percentage in height is also calculated from an average of three measurements.

### 2.3 Friction model in rigid-plastic finite element formulation

The general expression of constant shear friction model is Eq. 1.

$$\tau_s = mK \tag{1}$$

where  $\tau_s$  is the friction stress,  $m$  is the shear friction factor,  $0 \leq m \leq 1$ , and  $K$  is the shear yield stress.

In principle, friction modeling in the flow formulation of the rigid-plastic finite element method is expressed as follows [12, 16]:

$$\Pi = \int_V \bar{\sigma} \dot{\bar{\epsilon}} dV + \int_V \frac{\alpha}{2} \dot{\bar{\epsilon}}_v^2 dV + \int_{S_C} \left( \int_0^{|u_r|} \tau_s du_r \right) dS - \int_{S_F} T_i u_i dS \quad (2)$$

where  $\bar{\sigma}$  is the effective stress,  $\dot{\bar{\epsilon}}$  is the effective strain rate,  $\alpha$  is a large positive constant penalizing the volumetric strain rate component,  $\dot{\bar{\epsilon}}_v$  is a constraint on the kinematically admissible velocity fields in order to enforce the incompressibility,  $u_r$  is the relative velocity,  $S_C$  is the contact interface, and  $V$  is the control volume limited by the surfaces  $S_U$  and  $S_F$ , where velocity  $u_i$  and traction  $T_i$  are prescribed respectively.

Kobayashi et al. [28] presented that the unknown direction of the relative velocity between the die–workpiece interface for problems such as ring compression, rolling, and forging, and a unique feature of this type of problem is that there exists a point (or a region) along the die–workpiece interface where the velocity of the deforming material relative to the die becomes zero. The friction stress changes the direction at the neutral point, as shown in Fig. 3c. In order to avoid numerical problem in Eq. 2 due to abrupt changes in the friction stress near the neutral point, a

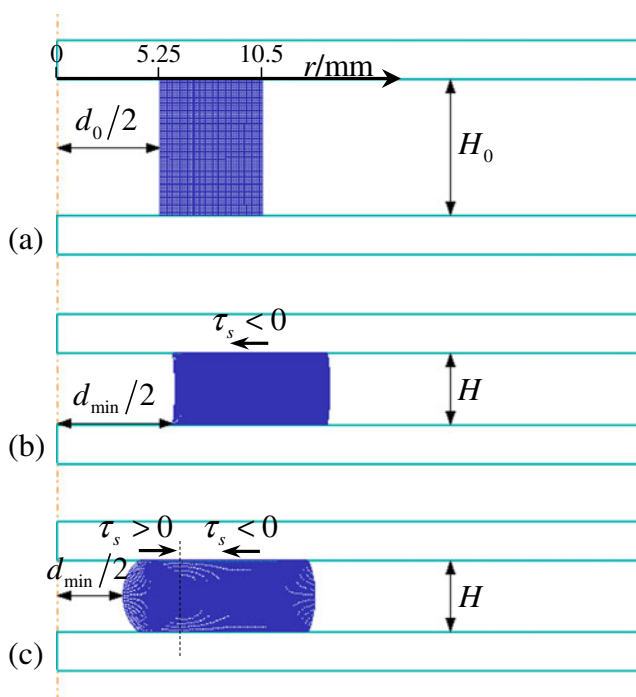


**Fig. 3** Geometry of ring in compressing process: **a** before compressing, **b** low friction, and **c** high friction

velocity-dependent friction stress expressed by Eq. 3 is used for the smooth transition of the friction stress in the range near the neutral point [12, 16, 28].

$$\tau_s = mK \left\{ \frac{2}{\pi} \arctan \left( \frac{|u_r|}{u_0} \right) \right\} \frac{u_r}{|u_r|} \quad (3)$$

where  $u_0$  is an arbitrary constant much smaller than relative velocity.

### 3 Results and discussion

#### 3.1 Friction calibration curves and friction factor

In the present study, the shear friction factor in the isothermal forming (high temperature) process of TA15 titanium alloy is measured by using the ring compression test. In order to obtain the value of the friction factor, the change in inner diameter of the compressed ring must be compared with the specific curves called calibration curves which are the predicted changes in the inner diameter under various friction factors. The friction calibration curves would be determined accurately by using FEM because the calibration curves can take into consideration the material properties, forming temperature ( $T$ ), loading speed ( $v$ ), etc.

The finite element analysis (FEA) is carried out by software package DEFORM. DEFORM provides four-node quadrilateral (two-dimensional model) or four-node tetrahedron element (three-dimensional model) to discretize deformable part. In the DEFORM package, the master/slave relationship is set for the contact pair. The initial element size is less than 0.1 mm for the ring (Fig. 3a which is based on the two-dimensional model), and the local mesh density is specified according to the mesh weighting factors for boundary curvature, strain, and strain rate when the ring is remeshed. The fine mesh can be obtained in the area with large boundary curvature, high strain, and high strain rate gradient. The relationship between stress and strain shown in Fig. 1 is used in the FEA.

The change in geometry of TA15 titanium alloy ring under the conditions such as friction factor, forming temperature, and loading speed can be predicted by means of the finite element method. According to FEM simulation results, the relationship (i.e., friction calibration curves) between the inner diameter (as shown in Fig. 3) and height of ring can be obtained. Then, the friction calibration curves can be elaborated according to the FEM results, and the friction factor can be obtained by comparing the experimental data with the corresponding calibration curves. The friction calibration curves and experimental results for TA15 titanium alloy isothermal

forming at  $T=970^{\circ}\text{C}$  under constant loading speed  $v=0.2\text{ mm/s}$  are shown in Fig. 4. Figure 4a shows a comparison between theoretical calibration curves and calibration curves elaborated by FEM, and the comparison indicates that there exist notable differences. The experimental results of TA15 titanium alloy ring compression test with lubricant 1, lubricant 2, and no lubricant under the conditions are shown in Fig. 4b. The  $m=0.5$  (with lubricant 1),  $m=0.19$  (with lubricant 2), and  $m=0.7$  (no lubricant) can be obtained by comparing the results with the FEM calibration curves.

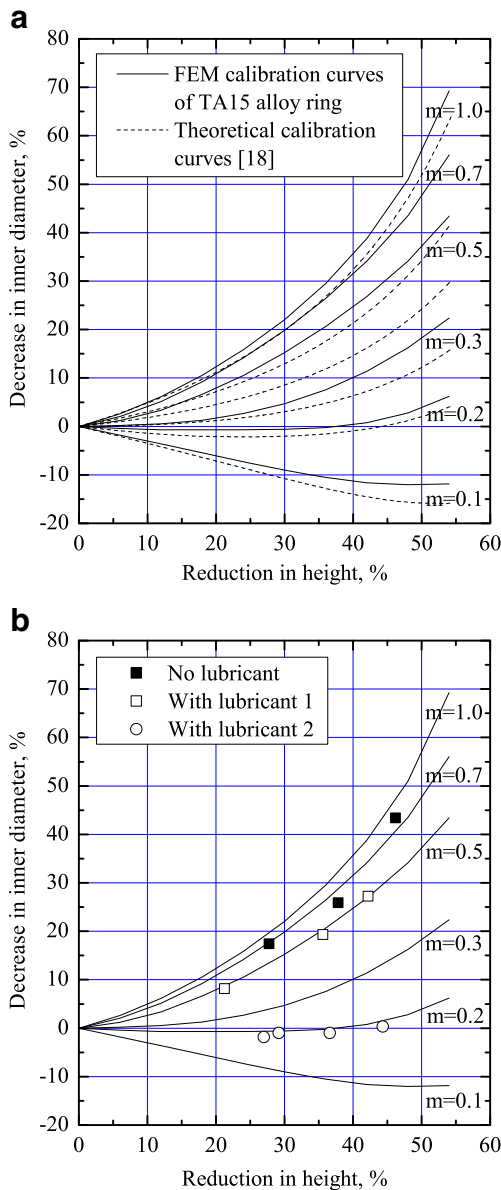


**Fig. 4** Friction calibration curves of TA15 titanium alloy ring for  $T=970^{\circ}\text{C}$ ,  $v=0.2\text{ mm/s}$ : **a** comparing with theoretical calibration curves and **b** experimental data of ring compression

### 3.2 Evaluation of measurement of friction factor

At  $T=970^{\circ}\text{C}$  and  $v=0.2\text{ mm/s}$ , results of the ring compression test with lubricant 1 and no lubricant are shown in Fig. 4b. The  $m=0.5$  under lubricated condition and  $m=0.7$  under unlubricated condition are obtained. Figure 5 illustrates forming load in the ring compression test and FEM simulation. There is a discrepancy between the simulation and experimental results, however the relative values are less than about 10%. It indicates that friction calibration curves elaborated in Section 3.1 are suitable for determining the friction factor, and the obtained friction factor is reasonable.

Large-scale complex component of TA15 titanium alloy with thin web and high rib can reduce the weight of the equipment and improve the performance. Isothermal local loading process provides an efficient way for near-net forming of these components with low force. The isothermal local loading forming process of one large-scale TA15 titanium alloy bulkhead (of which sizes in length and width are both greater than 1,000 mm) is carried out on an ordinary isothermal forging press. The upper die is divided into two parts (upper dies 1 and 2 as shown in Fig. 6), and the process has two local loading steps. In the first local loading step, the upper die 2 is higher than the upper die 1; thus, the load is almost applied to billet by upper die 1 although the upper dies 1 and 2 move simultaneously. In the second local loading step, the upper die 1 and the upper die 2 are at the same height and they also move simultaneously; the load is almost applied to the billet by the upper die 2 because the area under the upper die 1 has formed in the first loading step.

In the finite element model of the forming process of large-scale TA15 titanium alloy bulkhead, the constant shear friction model and the flow behavior (shown in Fig. 1) of TA15 titanium alloy are also used. The load of

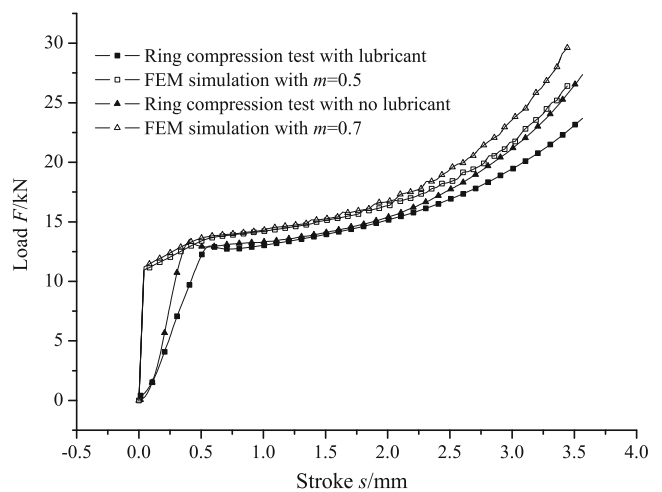


**Fig. 5** Stroke-load curves of ring compression

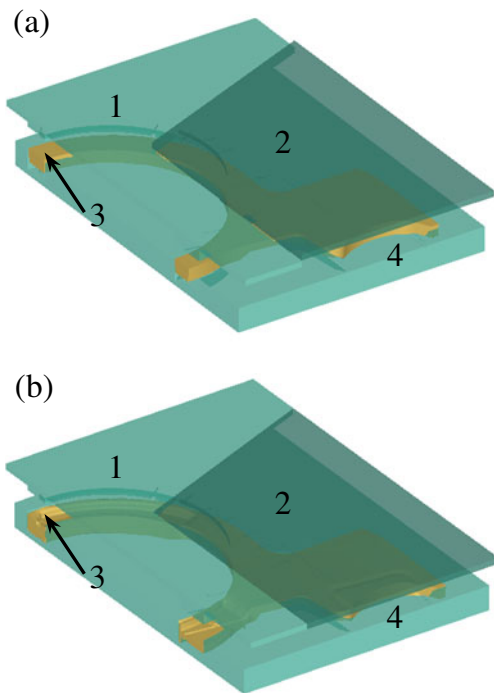


**Fig. 6** Local loading forming process of titanium alloy bulkhead; 1 upper die 1, 2 upper die 2, 3 billet/workpiece, 4 lower die: **a** first local loading step and **b** second local loading step

press in the second local loading is shown in Fig. 7. Not only the error between simulation and experiment is large but also the difference of changing tendency of forming load between simulation and experiment is large when the typical value (i.e.,  $m=0.3$  recommended by handbook) for lubricated hot forming processes is used in the simulation. However, the values and changing tendency show a good agreement with those in experiment when the determined value (i.e.,  $m=0.5$  measured in the present study) is used in the simulation. And the error of forming load can decrease

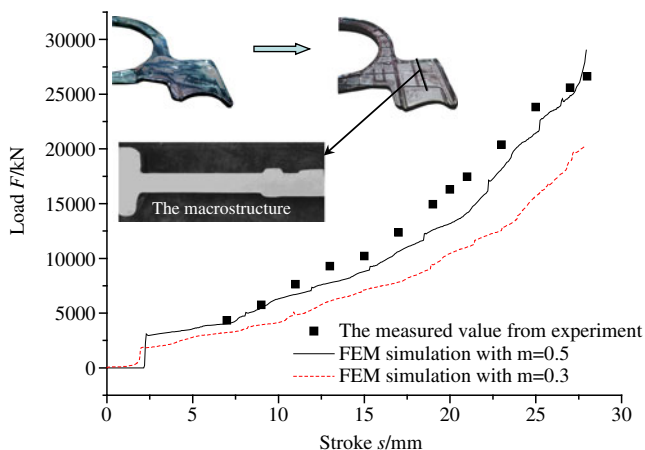


**Fig. 7** Forming load in second local loading step of TA15 bulkhead isothermal forging ( $T=970^{\circ}\text{C}$ ,  $v=0.2$  mm/s)

by about 5–25%. These also indicate that friction calibration curves elaborated in Section 3.1 are suitable for determining the friction factor and the obtained friction factor is reasonable. No defects about flow line, surface quality, and cavity fill are observed though poor lubrication ( $m=0.5$ ), as shown in Fig. 7, which means that the friction condition ( $m=0.5$ ) can satisfy the demands in industrial forming process.

### 3.3 Effect of loading speed and forming temperature

The friction calibration curves in Fig. 8 are elaborated according to the numerical results. Figure 8 illustrates the

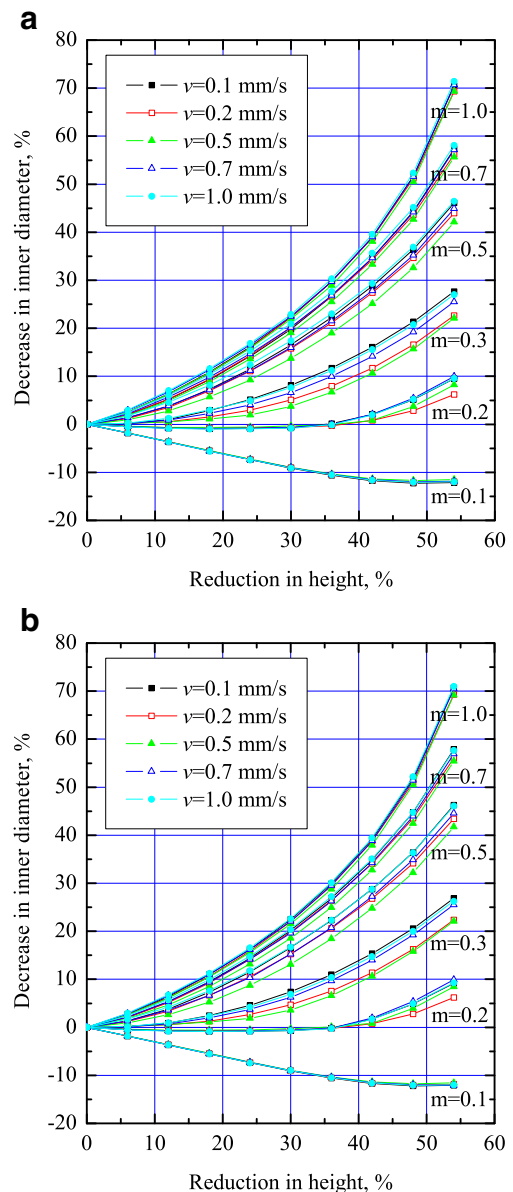


**Fig. 8** Friction calibration curves under different loading speeds: **a**  $T=950^{\circ}\text{C}$  and **b**  $T=970^{\circ}\text{C}$

friction calibration curves under different loading speeds. It can be seen from Fig. 8 that the loading speed makes a difference to the shape of the friction calibration curves, and the changes of calibration curves under  $T=970^{\circ}\text{C}$  are similar to those under  $T=950^{\circ}\text{C}$ . At the low ( $m$  less than about 0.1) friction condition or the high ( $m$  greater than about 0.7) friction condition, the influence of loading speed on the friction calibration curves can be ignored. However, in the midst magnitude of shear friction factors, such as about 0.2–0.5, the influence of loading speed is notable. Generally, when  $v=0.1\text{--}0.5$  mm/s, the calibration curves move downward with the increase of loading speed, i.e., the inner diameter of the ring is larger at larger speed if other conditions are not varied; when  $v=0.5\text{--}1.0$  mm/s, the inner diameter of the ring is smaller at larger speed if other conditions are not varied; and the shape of calibration curves is close to the shape of calibration curves at  $v=0.1$  mm/s with the increase of loading speed.

Hawkyard and Johnson [29] presented that the neutral layer may be within the material of the ring giving radially inward and outward flow (as shown in Fig. 3c), or it may be within the bore giving only outward (as shown in Fig. 3b). The volume of metal flowing inward and outward determines the inner diameter of the ring. Where the friction stress changes the direction is the position of neutral layer. The dependence of the friction shear stress along the interface (upper platen and ring) on loading speed is shown in Fig. 9, which is obtained by FEM. Of course, the shape of the barreled free surface (as shown in Fig. 3b, c) also affects the measured result.

It can be seen from Fig. 9 that the positions of the neutral layer under  $v=0.1, 0.5,$  and  $1.0$  mm/s are very close if other conditions are not varied. It means that loading speed has little influence on the volume of metal flowing inward and outward. The barrel is a reason for the laws occurring in Fig. 8. Ebrahimi and Najafizadeh [30] presented that the shape of the barrel is influenced by the initial height-to-diameter ratio and friction condition in cylinder upsetting, and the shape can be reasonably characterized as the arc of a circular curvature. In order to evaluate the degree of the barrel, a barrel parameter index  $k$  is determined and defined as:

$$k = \frac{d_{\max} - d_{\min}}{d_0} \tag{4}$$

If the volume of metal flowing inward is not varied, the measured inner diameter in Section 3.1 reduces with the increase in the barrel parameter index  $k$ . Figure 10 shows the  $k$  in different ring compression processes. The results indicate that the  $k$  under  $v=0.1, 0.5,$  and  $1.0$  mm/s are close when  $m=0.1$  and 0.7. However, when  $m=0.3$ , the  $k$  under  $v=0.5$  mm/s is less than the  $k$  under  $v=0.1$  and

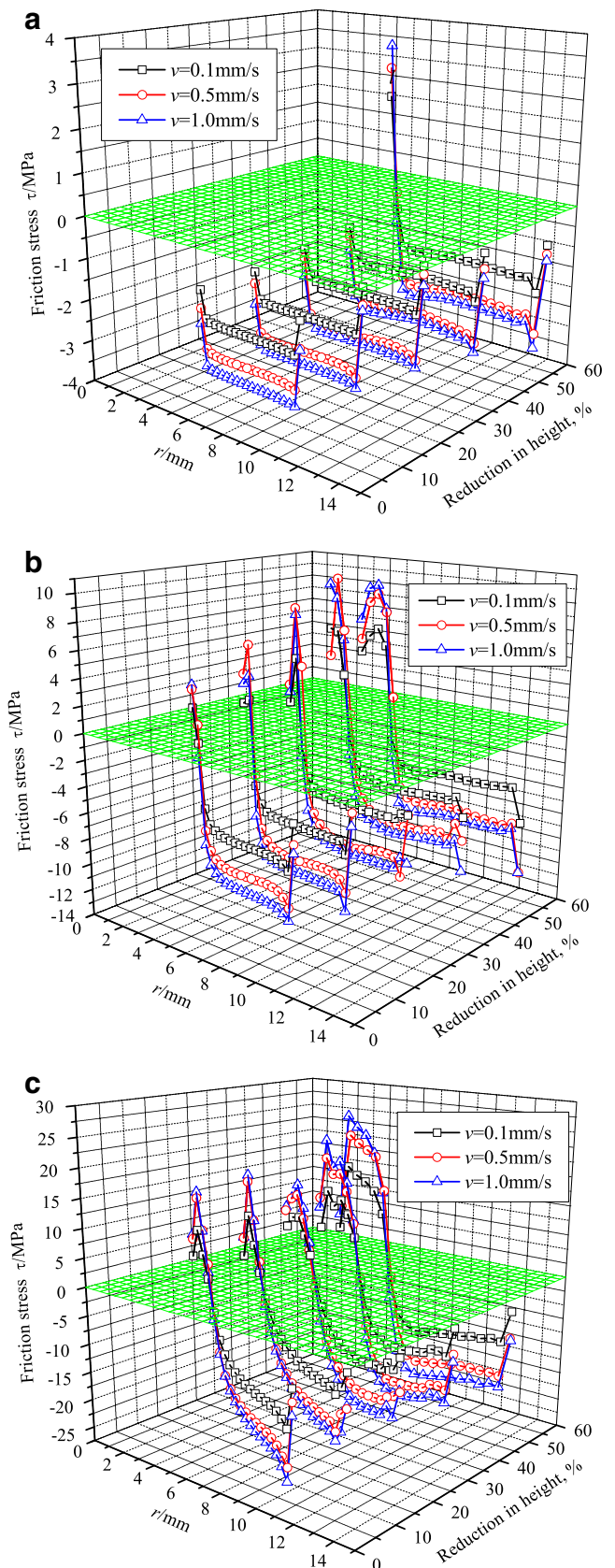


**Fig. 9** Distribution of frictional shear stress along die-workpiece interface ( $970^{\circ}\text{C}$ ): **a**  $m=0.1$ , **b**  $m=0.3$ , and **c**  $m=0.7$

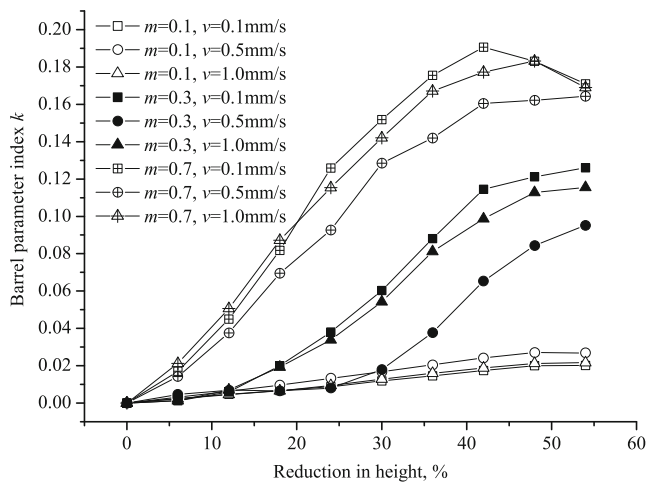


**Fig. 10** Barrel parameter index in different ring compression processes

1.0 mm/s which are close. Thus, the influence laws (shown in Fig. 8) of loading speed on friction calibration curves occur when  $v=0.1\text{--}1.0$  mm/s.

Figure 8 also illustrates the friction calibration curves under near-beta forging temperature ( $970^\circ\text{C}$ ) and conventional forging temperature ( $950^\circ\text{C}$ ). A temperature variation of  $20^\circ\text{C}$  has little influence on friction calibration curves, but it has a notable influence on lubricity of lubricant. The experimental results provide the support for it. At  $T=950^\circ\text{C}$  and  $v=0.2$  mm/s,  $m=0.7$  under unlubricated condition is also obtained from the ring compression test, but the value of the friction factor is about 0.4 (which decreases notably comparing with the value at  $T=970^\circ\text{C}$ ) by using lubricant 1. It can be seen from the geometry (shown in Fig. 11) of the ring after compression that the inner diameter under  $970^\circ\text{C}$  is less than that under  $950^\circ\text{C}$ . By using lubricant 2, the value of the factor is about 0.12 under  $950^\circ\text{C}$  which is less than  $m=0.16\text{--}0.20$  under  $970^\circ\text{C}$ , as shown in Fig. 12.



**Fig. 11** TA15 titanium alloy rings deformed to about 42% height reduction with lubricant 1: **a**  $T=950^\circ\text{C}$  and **b**  $T=970^\circ\text{C}$

The studies about graphite in the literature [22] presented that an increase of temperature causes the friction factor  $m$  to increase rapidly, and graphite loses almost all of its lubrication performance at  $1,000^\circ\text{C}$ . The graphite is added in lubricant 1 to decrease cost, and then the lubrication action decreases at elevated temperature, so the  $m$  by using lubricant 1 is greater than that by using lubricant 2. The experimental results [23] about glass indicate that  $m$  reduces with increase in temperature, but in temperatures above  $950^\circ\text{C}$ ,  $m$  increases with increase in temperature at strain rate  $0.05\text{ s}^{-1}$ . This phenomenon could be ascribed to that the glass possesses liquid characteristics as the temperature rises to  $950^\circ\text{C}$ , and then the molten glass is squeezed out of the interface at lower strain rate even with a recessed end specimen. Thus the lubrication action may decrease at temperatures above  $950^\circ\text{C}$ . As described in Section 2.2, the tests in the present study have a lower strain rate, so the  $m$  at  $970^\circ\text{C}$  is greater than that at  $950^\circ\text{C}$ .

According to the analysis about the influence of loading speed on calibration curves, the influence of loading speed on friction factor may be forecasted as following: (1) at the low ( $m$  less than about 0.1) or high ( $m$  greater than about 0.7) friction condition, the influence of loading speed on the friction factor can be ignored when  $v=0.1\text{--}1.0$  mm/s ( $\dot{\epsilon}=0.015\text{--}0.250\text{ s}^{-1}$ ) and (2) in the midst magnitude of shear friction factors, the value of  $m$  may decrease with the increase in loading speed when  $v=0.1\text{--}0.5$  mm/s, and the value of  $m$  may increase with the increase in loading speed when  $v=0.5\text{--}1.0$  mm/s. Figure 12 shows the friction factors under different loading speeds. Under unlubricated condition,  $m$  is about 0.7 under different speeds, and the maximum difference  $[(m_{\max}-m_{\min})/m_{\max}]$  of friction factors under different speeds is about 8%. When lubricant 2 is used at  $950^\circ\text{C}$ , the measured friction factor changes slightly at  $v=0.2, 0.5,$  and  $1.0$  mm/s, and the maximum difference under

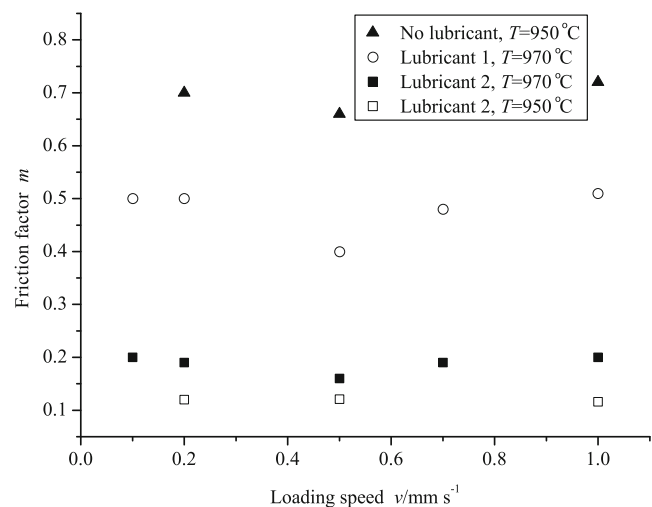


**Fig. 12** Friction factors under different loading speeds



different speeds is about 4%. In case when the lubricants 1 and 2 are used at 970°C, the friction factors are close at  $v=0.1$  and 1.0 mm/s, and the values at  $v=0.1, 0.2, 0.7,$  and 1.0 mm/s are greater than that at  $v=0.5$  mm/s. And the maximum differences under different speeds in these two cases are greater than 20%. The influence law is different from that the friction factor  $m$  decreases with the increase of strain rate declared by Li et al. [22, 23] which based on the results at strain rates 0.05, 0.5, 5, and 15  $s^{-1}$ .

At elevated temperature (above 950°C), Li et al. [22, 23] presented that the friction factor  $m$  decreases with the increase of strain rate. The main reasons for the phenomena are that the compression time affects the composition of lubricant and the weight of the lubricant between the die and ring which decide lubricity of the lubricant film. The glass softens sufficiently to possess liquid characteristics as the temperature rises to 950°C. The engine oil in which the graphite dispersed decomposes at elevated temperature (above 750°C), and organic vapors discharged in the decomposing process are the main vapors absorbed onto the graphite platelets. At lower strain rate (0.05  $s^{-1}$ ), the compression time is long, then the molten glass is squeezed out, and more vapors absorbed onto the graphite are piled out. Thus lubrication action is decreased. The compression time is shortened by increasing strain rate (0.5, 5, 15  $s^{-1}$ ), then the glass being squeezed out and the vapor being piled out are reduced, and thus lubrication action increases. However, the strain rates in all tests of this study are around 0.05  $s^{-1}$ . The composition of the lubricant and the weight of lubricant changed little in this range of loading speeds. According to analyses about Figs. 9 and 10, the main reason for the influence law of loading speed in the present study is that the loading speed affects the shape of barreled free surface. Radial velocity of metal flow is nonuniform due to frictional resistance at die–workpiece interface, and thus the free surface of the ring would barrel as shown in Fig. 3. Effect of frictional resistance would gradually reduce with the decrease in friction factor, and then the nonuniform metal flow reduces (i.e., value of  $k$  reduces). Thus, the influence of loading speed on barrel parameter index  $k$  is not notable under low friction condition ( $m$  less than about 0.1) and low loading speed (0.1–1.0 mm/s). Moreover, under high friction condition ( $m$  greater than about 0.7) and the low loading speed, the influence of frictional resistance on  $k$  is greater than the influence of loading speed, and thus influence of loading speed on  $k$  is also not notable.

#### 4 Conclusions

1. The friction calibration curves for  $m$  are elaborated by using the finite element method, in which the material property and forming conditions are considered. Combining isothermal ring compression test, the shear friction factor in isothermal forming of TA15 titanium alloy is evaluated. In isothermal forging process of TA15 titanium alloy under  $v=0.1$ –1.0 mm/s, shear friction factor  $m$  is about 0.16–0.50 at 970°C and 0.12–0.40 at 950°C with glass lubricants.
2. The influence of loading speed on  $m$  is similar to that on friction calibration curves. At the low ( $m$  less than about 0.1) or high ( $m$  greater than about 0.7) friction condition, the influence can be ignored. However, in the midst magnitude of shear friction factors, the inner diameter of the ring increases when  $v=0.1$ –0.5 mm/s and reduces when  $v=0.5$ –1.0 mm/s with the increase in loading speed. It means that  $m$  decreases at first and then increases from 0.1 to 1.0 mm/s.
3. The temperature at 950°C and 970°C has little influence on the friction calibration curves, but it has a notable influence on lubricity of the lubricant. The  $m$  under lubricated condition increases with the increase in temperature.

**Acknowledgments** The authors would like to gratefully acknowledge the supports of the National Natural Science Foundation for Key Program of China (Grant No. 50935007), the National Basic Research Program of China (973 Program, Grant No. 2010CB731701), and the 111 Program (Grant No. B08040).

#### References

1. Leyens C, Peters M (2003) Titanium and titanium alloys. Wiley-VCH, Weinheim
2. Lütjering G, Williams JC (2007) Titanium, 2nd edn. Springer, Heidelberg
3. Yang H, Fan XG, Sun ZC, Guo LG, Zhan M (2011) Recent developments in plastic forming technology of titanium alloys. Sci China Tech Sci 54(2):490–501
4. Shen G, Furrer D (2000) Manufacturing of aerospace forging. J Mater Process Tech 98:189–195
5. Bewlay BP, Gigliotti MFX, Utyashev FZ, Kaibyshev OA (2000) Superplastic roll forming of Ti alloys. Mater Des 21:287–295
6. Yeom JT, Kim JH, Park NK, Choi SS, Lee CS (2007) Ring-rolling design for large-scale ring product of Ti–6Al–4V alloy. J Mater Process Tech 187–188:747–751
7. Kong TF, Chan LC, Lee TC (2008) Numerical and experiment investigation perform design in non-axisymmetric warm forming. Int J Adv Manuf Tech 37:908–919
8. Hussain G, Gao L, Zhang ZY (2008) Formability evaluation of a pure titanium sheet in cold increment forming process. Int J Adv Manuf Tech 37:920–926
9. Shan D, Yang G, Xu W (2009) Deformation history and the resultant microstructure and texture in backward tub spinning of Ti–6Al–2Zr–1Mo–1V. J Mater Process Tech 209:5713–5719
10. He DH, Li DS, LI XQ, Jin CH (2010) Optimization on springback reduction in cold stretch forming of titanium-alloy aircraft skin. Trans Nonferrous Met Soc China 20:2350–2357
11. Kalpakjiana S (1985) Recent progress in metal forming tribology. Ann CIRP 34(2):585–592

12. Tan X (2002) Comparisons of friction models in bulk metal forming. *Tribol Int* 35:385–393
13. Malayappan S, Narayanasamy R (2004) An experiment analysis of upset forging of aluminium cylindrical billets considering the dissimilar friction conditions at flat die surface. *Int J Adv Manuf Tech* 23:636–643
14. Menezes PL, Kishore KK, Kailas SV (2009) Influence of friction during forming process—a study using a numerical simulation technique. *Int J Adv Manuf Tech* 40:1067–1076
15. Joun MS, Moon HG, Choi IS, Lee MC, Jun BY (2009) Effects of friction laws on metal forming processes. *Tribol Int* 42:311–319
16. Petersen SB, Martins PAF, Bay N (1997) Friction in bulk metal forming: a general friction model vs. the law of constant friction. *J Mater Process Tech* 66:186–194
17. Altan T, Oh SI, Gegel HL (1983) *Metal forming: fundamentals and application*. American Society for Metals, Metal Park
18. Mielnik EM (1991) *Metalworking science and engineering*. McGraw-Hill, New York
19. Sofuoglu H, Rasty J (1999) On the measurement of friction coefficient utilizing the ring compression test. *Tribol Int* 32:327–335
20. Fereshteh-Saniee F, Pillinger I, Hartley P (2004) Friction modelling for the physical simulation of the bulk metal forming processes. *J Mater Process Tech* 153–154:151–156
21. Rudkins NT, Hartley P, Pillinger I, Petty D (1999) Friction modelling and experimental observations in hot ring compression tests. *J Mater Process Tech* 60:349–353
22. Li LX, Peng DS, Liu JA, Liu ZQ (2001) An experiment study of the lubrication behavior of graphite in hot compression tests of Ti–6Al–4V alloy. *J Mater Process Tech* 112:1–5
23. Li LX, Peng DS, Liu JA, Liu ZQ, Jiang Y (2000) An experiment study of the lubrication behavior of A5 glass lubricant by means of the ring compression tests. *J Mater Process Tech* 102:138–142
24. Shen CW (2007) *Research on material constitution models of TA15 and TC11 titanium alloys in hot deformation processes*. Master thesis, Northwestern Polytechnical University (in Chinese)
25. Zhang DW, Yang H, Sun ZC (2010) Analysis of local loading forming for titanium-alloy T-shaped components using slab method. *J Mater Process Tech* 210:258–266
26. Sun Z, Yang H (2009) Microstructure and mechanical properties of TA15 titanium alloy under multi-step local loading forming. *Mater Sci Eng A* 523:184–192
27. Wang SL, Ruan XY, Yu XL, Chen SC, Hu ZS (1996) A research on constitutive equations for hot workings of metals. *J Shanghai Jiaotong Univ* 30(8):20–14, in Chinese
28. Kobayashi S, Oh SI, Altan T (1989) *Metal forming and the finite-element method*. Oxford University Press, New York
29. Hawkyard JB, Johnson W (1967) An analysis of the changes in geometry of a short hollow cylinder during axial compression. *Int J Mech Sci* 9(4):163–182
30. Ebrahimi R, Najafizadeh A (2004) A new method for evaluation of friction in bulk metal forming. *J Mater Process Tech* 152:136–143